Mon. Not. R. Astron. Soc. **000**, 1–8 (2008) Printed 16 February 2009 (MN LaTeX style file v2.2)

arXiv:0902.2597v1 [astro-ph.CO] 16 Feb 2009

# Radiative Regulation of Population III Star Formation

K. Hasegawa [1]⋆ , M. Umemura[1] and H. Susa[2] ⋆
[1] *Center for Computational Sciences, University of Tsukuba, Ten-nodai, 1-1-1 Tsukuba, Ibaraki 305-8577, Japan*
[2] *Department of Physics, Konan University, Japan*

Accepted 1988 December 15. Received 1988 December 14; in original form 1988 October 11

**ABSTRACT**
We explore the impact of ultraviolet (UV) radiation from massive Population III (Pop III) stars of 25, 40, 80, and 120 $M_\odot$ on the subsequent Pop III star formation. In this paper, particular attention is paid to the dependence of radiative feedback on the mass of source Pop III star. UV radiation from the source star can work to impede the secondary star formation through the photoheating and photodissociation processes. Recently, Susa & Umemura (2006) have shown that the ionizing radiation alleviates the negative effect by $H_2$-dissociating radiation from $120M_\odot$ PopIII star, since an $H_2$ shell formed ahead of an ionizing front can effectively shield $H_2$-dissociating radiation. On the other hand, it is expected that the negative feedback by $H_2$-dissociating radiation can be predominant if a source star is less massive, since a ratio of the $H_2$-dissociating photon number to the ionizing photon number becomes higher. In order to investigate the radiative feedback effects from such less massive stars, we perform three-dimensional radiation hydrodynamic simulations, incorporating the radiative transfer effect of ionizing and $H_2$-dissociating radiation. As a result, we find that if a source star is less massive than $\approx 25M_\odot$, the ionizing radiation cannot suppress the negative feedback of $H_2$-dissociating radiation. Therefore, the fate of the neighboring clouds around such less massive stars is determined solely by the flux of $H_2$-dissociating radiation from source stars. With making analytic estimates of $H_2$ shell formation and its shielding effect, we derive the criteria for radiation hydrodynamic feedback depending on the source star mass.

**Key words:** early universe - galaxies: formation - radiative transfer - hydrodynamics

## 1 INTRODUCTION

The reionization and metal enrichment of the universe are thought to begin with the formation of first metal-free (Pop III) stars (Gnedin 2000; Ciardi et al. 2001; Cen 2003; Sokasian et al. 2004). Hence, the formation rate of Pop III stars is crucial for the subsequent structure formation in the universe. The Pop III objects are expected to collapse at $20 \lesssim z \lesssim 30$, forming a minihalo with a mass of $\approx 10^6 M_\odot$ and an extent of $\approx$ 100pc (Tegmark et al. 1997; Fuller & Couchman 2000; Yoshida et al. 2003). In the course of bottom-up structure formation, such Pop III minihaloes merge to form first galaxies at $z \gtrsim 10$, having the virial temperature $T_{\rm vir} \gtrsim 10^4$K and the mass $\gtrsim 10^8 M_\odot$. Even in the evolution of first galaxies, Pop III stars can play a significant role, since an appreciable number of stars may form from metal-free component in interstellar gas (Tornatore et al. 2007; Johnson et al. 2008).

The formation of very first stars has been investigated intensively in the last decade. Many studies have come to a similar conclusion that such stars form in a top-heavy mass function with the peak of $\approx 100M_\odot$ (e.g., Abel, Bryan & Norman 2000; Bromm, Coppi & Larson 2002; Nakamura & Umemura 2001; Yoshida et al. 2006). Recently, O'Shea & Norman (2007) have shown that the variations of cosmological density fluctuations allow the mass of Pop III stars to be down to $\sim 20M_\odot$.

On the other hand, the secondary Pop III star formation has been investigated recently. The formation of secondary stars is subject to various feedback effects by first stars. One of them is the supernova (SN) feedback through mechanical and chemical effects. The negative feedback by SNe is the evaporation of neighboring clouds, since the SN shock heats up the gas in clouds. On the hand, SNe can bring positive feedback through the compression by shock and the cooling by ejected heavy elements. The secondary star formation can be promoted by such positive feedback effects (Mori et al. 2002; Bromm et al. 2003; Kitayama & Yoshida 2005; Greif et al. 2007). Another important feedback effect is brought by the ultraviolet (UV) radiation from first stars, since they are very luminous at ultraviolet band. First stars

---

⋆ E-mail: hasegawa@ccs.tsukuba.ac.jp (KH); umemura@ccs.tsukuba.ac.jp (UM); susa@konan-u.ac.jp (HS)

photoionize and photoheat the surrounding media, and also photodissociate $H_2$ molecules, which are the main coolant of primordial gas. The radiative feedback from first stars is the primary feedback until first stars end the life-time of $\sim 10^6$yr with SNe.

The photodissociation of $H_2$ molecules leads to a negative radiative feedback effect, which has been studied by many authors so far. Omukai & Nishi (1999) investigated the effect of $H_2$-dissociating radiation from a single Pop III star residing in a virialized halo. They found that if the halo is uniform, $H_2$ molecules in the halo are totally dissociated, so that the gas cannot collapse to form stars. Glover & Brand (2001) considered more realistic clumpy halos. They found that if the gas density is sufficiently high, photodissociation process proceeds slower than the collapse of the cloud. Hence, the cloud can form stars. This result is confirmed by the recent 3D radiation hydrodynamic simulation by Susa (2007) including the effects of hydrodynamics as well as the radiation transfer of $H_2$-dissociating radiation. The feedback effects by diffuse $H_2$-dissociating radiation can be important after the local feedback in minihaloes (Haiman, Rees & Loeb 1997; Machacek, Bryan & Abel 2001; Yoshida et al. 2003; O'Shea & Norman 2008).

These works basically focused on the photodissociation effects. We also have to take into account the effects of ionizing photons. Ionizing radiation heats up the gas through the photoionization processes. The temperature of photoheated gas is kept to be around $10^4$K, owing to the balance between the radiative cooling and photoheating. If the gravitational potential of star forming halos are not so deep as to retain the photoheated gas, the heated gas evaporates from the halos (e.g., Susa & Umemura 2004a,b; Yoshida et al. 2007b; Wise & Abel 2008; Whalen et al. 2008). However, the case in which ionizing radiation is coupled with $H_2$-dissociating radiation is complex. When an ionization front (I-front) propagates in a collapsing core, the enhanced fraction of electrons catalyzes $H_2$ formation (Shapiro & Kang 1987; Kang & Shapiro 1992; Susa et al. 1998; Oh & Haiman 2002). In particular, the mild ionization ahead of the I-front generates an $H_2$ shell, which potentially shields $H_2$ dissociating photons (Ricotti, Gnedin, & Shull 2001). This mechanism is likely to work positively to form Pop III stars. On the other hand, the I-front can be accompanied with a shock for an optically-thick cloud (Susa & Umemura 2006). The shock affects significantly the collapse of cloud. This is a totally radiation hydrodynamic (RHD) process. Such radiation hydrodynamic feedback has been investigated by 1D spherical RHD simulations (Ahn & Shapiro 2007), 2D cylindrical RHD simulations (Whalen et al. 2008), and 3D RHD simulations (Susa & Umemura 2006). The results by 2D and 3D simulations are in good agreement with each other. It is found that ionizing radiation can bring positive feedback through the formation of $H_2$ shell.

Susa & Umemura (2006) investigated RHD feedback by a $120M_\odot$ source star, and Susa, Umemura & Hasegawa (2008) derived the feedback criterion. However, if a source star is less massive, the relative intensity of $H_2$-dissociating radiation to ionizing radiation increases. Then, the feedback tends to be more negative. In fact, the mass of first stars might be some $10M_\odot$ owing to the variations of cosmological density fluctuations (O'Shea & Norman 2007), the enhanced $H_2$ cooling in pre-ionized gas (Shapiro & Kang 1987; Susa et al. 1998; Oh & Haiman 2002), or the HD cooling in fossil HII regions (e.g., Uehara & Inutsuka 2000; Nakamura & Umemura 2002; Nagakura & Omukai 2005; Johnson & Bromm 2006; Greif & Bromm 2006; Yoshida, Omukai & Hernquist 2007a). Also, the elemental abundance patterns of hyper-metal-poor stars well match the yields by supernova explosions with a progenitor mass of $\sim 25M_\odot$ (Umeda & Nomoto 2003; Iwamoto et al. 2005). The RHD feedback effects by Pop III stars less massive than $100M_\odot$ have not been investigated so far, and no criterion has not been derived.

**Table 1.** Properties of Pop III source stars

| Mass | $T_{\rm eff}$ [K] | $\dot{N}_{\rm ion}$ [s$^{-1}$] | $L_{\rm LW}$[erg/s] |
|---|---|---|---|
| $120M_\odot$ | $9.57 \times 10^4$ | $1.069 \times 10^{50}$ | $5.34 \times 10^{23}$ |
| $80M_\odot$ | $9.33 \times 10^4$ | $5.938 \times 10^{49}$ | $3.05 \times 10^{23}$ |
| $40M_\odot$ | $7.94 \times 10^4$ | $1.873 \times 10^{49}$ | $1.17 \times 10^{23}$ |
| $25M_\odot$ | $7.08 \times 10^4$ | $5.446 \times 10^{48}$ | $3.94 \times 10^{22}$ |

In this paper, we perform 3D RHD simulations in order to investigate the radiative feedback effects from Pop III stars with various masses. We derive the criteria for the collapse of cloud cores irradiated by a neighboring Pop III star with 25,40,80, or $120M_\odot$. In §2, the simulation code and procedure are described. The simulation results are presented in §3. Finally, we summarize the conclusions in §4.

## 2 SIMULATION CODE AND PROCEDURE

We perform RHD simulations with a 3D Radiation-SPH code developed by ourselves. In the code, we treat self-consistently the gravitational force, hydrodynamics, the radiative transfer of UV photons, non-equilibrium chemistry for $e^-$, $H^+$, H, $H^-$, $H_2$, and $H_2^+$. We use the chemical network solver in Kitayama et al. (2001) as well as the radiative transfer solver described in Susa (2006). For the shielding by $H_2$ molecules against $H_2$-dissociating radiation at Lyman-Werner (LW) band (11.26-13.6 eV), we employ the self-shielding function introduced by Draine & Bertoldi (1996). The opacity against LW band flux ($F_{\rm LW}$) is calculated by

$$F_{\rm LW} = F_{\rm LW,0} f_{\rm s}\left(N_{\rm H_2,14}\right) \tag{1}$$

where $F_{\rm LW,0}$ is the incident flux, $N_{\rm H_2,14}$ is the $H_2$ column density in units of $10^{14}{\rm cm}^{-2}$, and

$$f_{\rm s}(x) = \begin{cases} 1, & x \leqslant 1 \\ x^{-3/4}, & x > 1 \end{cases} \tag{2}$$

In this paper, we simulate the evolution of a purely baryonic primordial cloud, according with the model by Susa & Umemura (2006). The cloud is initially uniform with the density of $n_{\rm H} = 14{\rm cm}^{-3}$, and has the mass of $M = 8.3 \times 10^4 M_\odot$. The initial chemical compositions are assumed to be the cosmological compositions provided by Galli & Palla (1998). Before the UV irradiation, the cloud contracts self-gravitationally to form a collapsing core. As for the core temperature $T_{\rm c}$, we employ two models. One is a high temperature model, and the other is a low temperature model. By changing the initial temperature of the

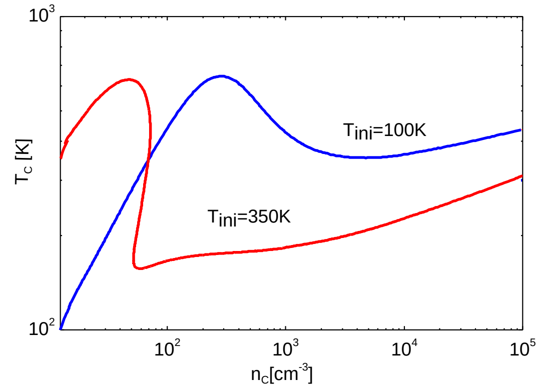

**Figure 1.** Evolution of the core without radiative feedback. The time variations of core temperature are shown for the initial temperature 350K (red curve) and 100K (blue curve), respectively.

clouds $T_{\rm ini}$, we realize such core temperatures. As shown in Fig. 1, if we set $T_{\rm ini} = 100$K, the core temperature becomes $T_{\rm c} \sim 300-400$K at core density $n_{\rm c} \gtrsim 10^2{\rm cm}^{-3}$. On the other hand, if the initial temperature is set to be $T_{\rm ini} = 350$K, the cloud core cools below $T_{\rm c} \sim 200$K, since $H_2$ molecules are rapidly formed owing to the high initial temperature (see Fig.1). Another difference between two models is the ratio of gravitational energy $W$ to internal energy $U$, because it is dependent on the initial temperature. The $|W|/U$ ratio is $\approx 4$ for the low initial temperature (high $T_{\rm c}$) model, while the $|W|/U$ ratio is $\approx 2$ for the high initial temperature (low $T_{\rm c}$) model.

We ignite a source star when the density of cloud core exceeds a certain value $n_{\rm on}$. The source star is placed $D$ pc away from the center of cloud core. We change the mass of source star in the range of $25M_\odot \leqslant M_* \leqslant 120M_\odot$. The properties of source stars as the effective temperature of star $T_{\rm eff}$, the number of ionizing photons emitted per second $\dot{N}_{\rm ion}$, and the luminosity at LW band are taken from Schaerer (2002), which are summarized in Table 1. Note that we do not consider the lifetimes of source stars in this paper, since we focus on elucidating the RHD feedback before SN explosions.

Numerical runs are characterized by the parameters $D$, $n_{\rm on}$, and $M_*$. The simulations are performed until $t_{\rm end} = 2t_{\rm ff}$, where $t_{\rm ff}$ is the free-fall time determined by $n_{\rm on}$. If the density of cloud core exceeds $5 \times 10^5{\rm cm}^{-3}$ before $t_{\rm end}$, we stop the calculation, since the cloud is expected to keep collapsing. In order to clarify the effects of the ionizing radiation, we also perform the simulations artificially disregarding ionizing radiation but still including LW radiation, and the results are compared with those of normal simulations. The number of SPH particles handled in our simulations is 262,144 for all runs.

The present simulations are mainly carried out with a novel hybrid computer system in University of Tsukuba, called *FIRST* simulator, which has been designed to simulate multi-component self-gravitating radiation hydrodynamic systems with high accuracy (Umemura et al. 2007). The *FIRST* simulator is composed of 256 nodes with dual Xeon processors, and each node possesses a Blade-GRAPE board, on which GRAPE-6 chips, that is, the accelerator of gravity calculations, are implemented. The peak performance of *FIRST* simulator is 36.1 Tflops.

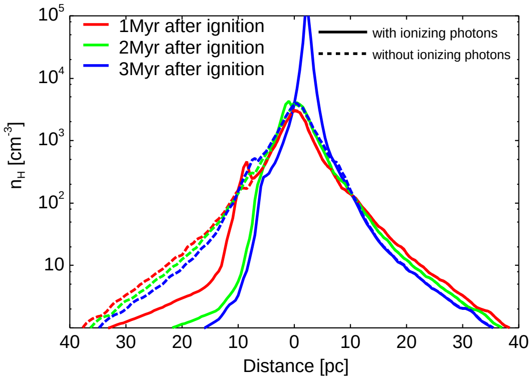

**Figure 2.** Time variations of density profiles along the symmetry axis for a simulation with $T_{\rm c} \sim 400$K, $M_* = 80M_\odot$, $n_{\rm on} = 10^3{\rm cm}^{-3}$, and $D = 40$pc. The red, green, and blue lines represent the profiles at 1Myr, 2Myr, and 3 Myr after the ignition, respectively. The results without ionizing radiation are shown by dashed lines. It is shown that the core cannot collapse without ionizing radiation.

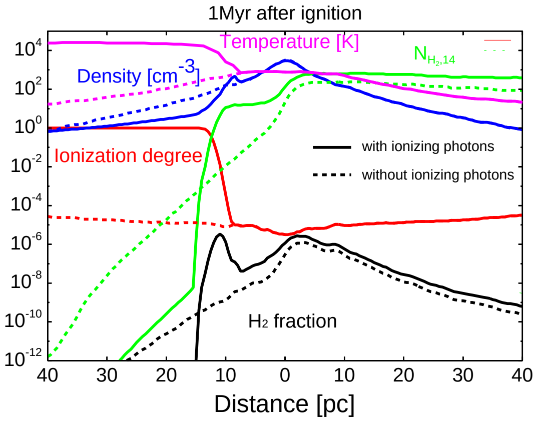

**Figure 3.** Various physical quantities along the symmetry axis at 1Myr after the ignition for the simulation shown in Fig. 2. The results with and without ionizing radiation are shown by solid and dashed lines, respectively. The magenta, blue, red, green, and black lines show the gas temperature(K), number density (${\rm cm}^{-3}$), electron fraction, $H_2$ column density from the source star in units of $10^{14}{\rm cm}^{-2}$, and the $H_2$ fraction, respectively.

## 3 TYPICAL RESULTS

In this section, we show the typical evolution of clouds. For a high core temperature model ($T_{\rm c} \sim 300-400$K), the time evolution of density profiles along the symmetry axis is shown in Fig. 2, where the set-up parameters are $M_* = 80M_\odot$, $n_{\rm on} = 10^3{\rm cm}^{-3}$, and $D = 40$pc. In this figure, the results with ionizing radiation are compared to those without ionizing radiation. In the simulation with ionizing radiation, the density of cloud core keeps increasing, and the density exceeds the limit ($5 \times 10^5{\rm cm}^{-3}$) due to the run-away collapse at 3.4Myr after the ignition of the source star. On the other hand, in the simulation without ionizing radiation, the gravitational contraction of cloud core is stopped by the thermal pressure, and eventually a hydrostatic core forms.

Various physical quantities along the symmetry axis at 1Myr are shown in Fig. 3. If ionizing radiation is included, a dense shell forms ahead of the ionization front (I-front) . The

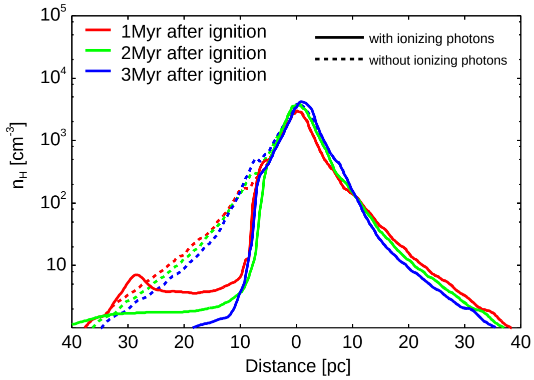

**Figure 4.** Same as Fig. 2, but for $M_* = 25M_\odot$. $D = 14$pc is set up so that the LW band flux toward the cloud core should be the same as Fig. 2.

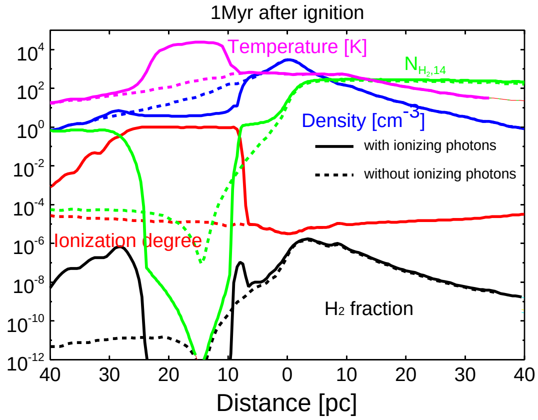

**Figure 5.** Same as Fig. 3, except that the parameters are $M_* = 25M_\odot$ and $D = 14$pc.

$H_2$ molecule fraction is raised up to a level $y_{H_2} \approx 10^{-5}$ in the shell, so that $H_2$ column density exceeds $10^{14}\mathrm{cm}^{-2}$. Owing to the self-shielding of LW band radiation by the shell, the $H_2$ fraction in the cloud core is increased, compared to the case without ionizing radiation. Eventually, the enhanced $H_2$ cooling allows the core to undergo the run-away collapse. On the other hand, unless ionizing radiation is included, LW band radiation from the source star reduces the $H_2$ fraction, so that the cloud core is settled in a hydrostatic configuration. This mechanism is basically the same as that found by Susa & Umemura (2006); Susa, Umemura & Hasegawa (2008) in the case of $M_* = 120M_\odot$ .

In Fig. 4 and Fig. 5, the results in the case of $M_* = 25M_\odot$ are shown, where $n_{\rm on} = 10^3\mathrm{cm}^{-3}$. Here, the source distance is set to be $D = 14$pc so that the LW band flux toward the cloud core should be the same as that in the case of $M_* = 80M_\odot$, whereas the flux of ionizing radiation is about 0.75 times weaker than that in the $M_* = 80M_\odot$ case. As shown in Fig. 4, the cloud fails to collapse and a hydrostatic core forms, notwithstanding the presence of ionizing radiation. Similar to the case of $M_* = 80M_\odot$, the $H_2$ fraction ahead of the I-front is enhanced associated with a dense shell. However, the $H_2$ column density of the shell is not high enough to shield the $H_2$ dissociating photons. Thus, the $H_2$ fraction at the cloud core stays as low as $y_{H_2} \approx 10^{-6}$, which is the almost same level in the case without ionizing radiation. Thus, in this lower stellar mass case, the ionizing radiation cannot suppress the negative feedback.

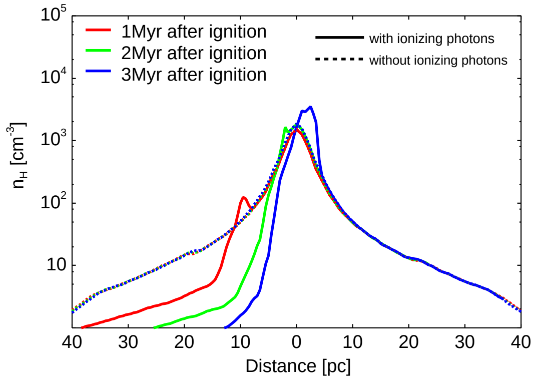

**Figure 6.** Same as Fig. 2, but for $T_c \sim 200$K.

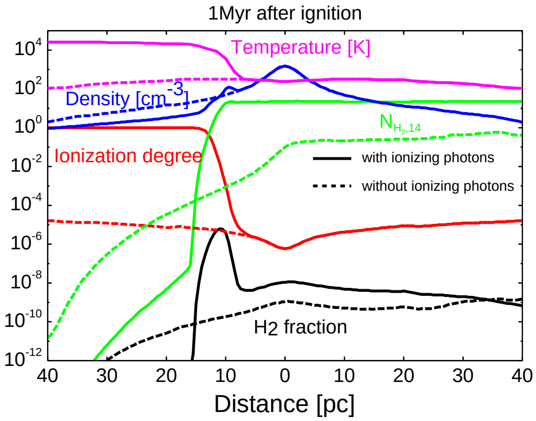

**Figure 7.** Same as Fig. 3, but for $T_c \sim 200$K.

In Fig. 6 and Fig. 7, the results for the low core temperature model ($T_c \sim 200$K) are shown. In these simulations, the parameters are set to be $M_* = 80M_\odot$, $D = 40$pc, and $n_{\rm on} = 10^3\mathrm{cm}^{-3}$. As shown in Fig. 6, the cloud fails to collapse, despite the presence of ionizing radiation. However, the reason for the failure is different from the $M_* = 25M_\odot$ case. It can be seen in Fig. 7 that the shielding effect raises the $H_2$ column density, compared to the case with no ionizing radiation. In this low core temperature model, hydrogen molecules are strongly destroyed by the LW radiation, and the $H_2$ fraction decreases to $y_{H_2} \approx 10^{-8}$. Since the core radius is smaller for the low core temperature, the self-shielding for LW radiation by the core is weaker.

## 4 CRITERIA FOR RADIATIVE FEEDBACK

### 4.1 Numerical Criteria

In Fig. 8, the numerical results are summarized for a high core temperature model ($T_c \sim 300-400$K). In this figure, crosses denote the failed collapse, triangles represent the successful collapse with the aid of ionizing radiation, and circles represent the collapse regardless of ionizing radiation. As shown in this figure, in the simulation runs with $M_* \geqslant 40M_\odot$, the $H_2$ shell driven by ionizing radiation can

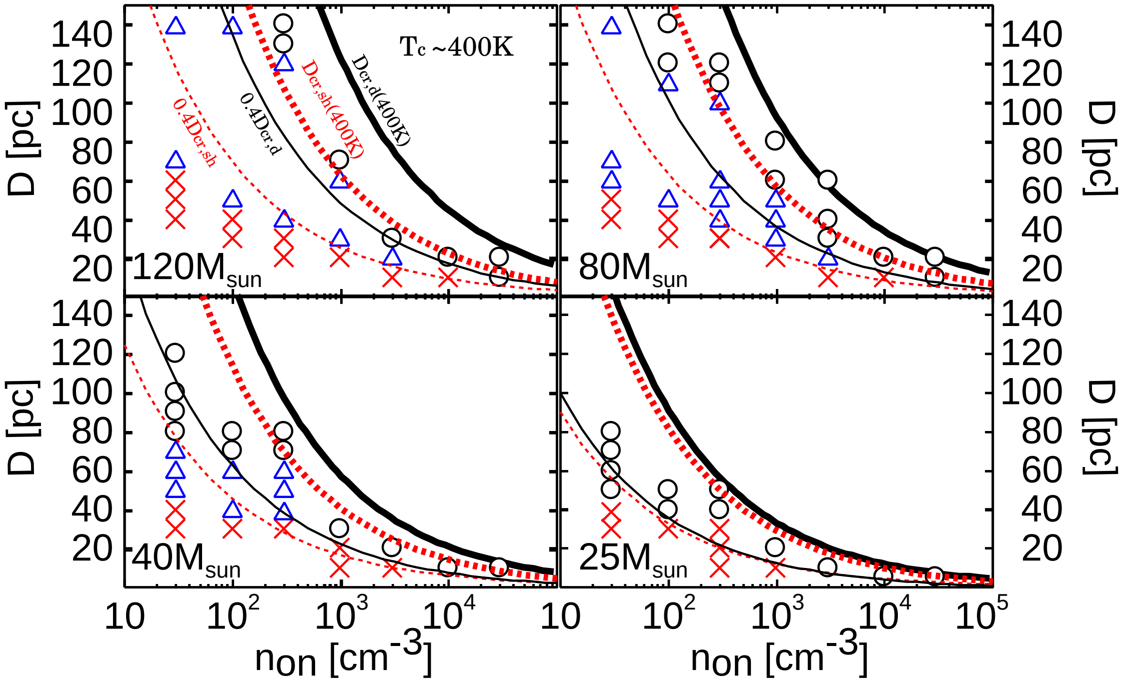

**Figure 8.** Numerical results for $T_c \sim 400$K are summarized in terms of $D$ and $n_{\rm on}$. From the top-left panel to the bottom-right panel, each panel represents the result with $M_* = 120M_\odot$, $80M_\odot$, $40M_\odot$, and $25M_\odot$. Crosses denote the runs in which the clouds fail to collapse, triangles represent the runs in which the clouds can collapse if the ionizing radiation is included, and circles represent the runs in which the clouds can collapse even if the ionizing radiation is not included. Thick solid lines indicate the analytic criteria $D_{\rm cr,d}$, which is derived from balancing photodissociation timescale to free-fall timescale (see the text for the detail). On the other hand, dotted lines indicate the analytic criteria $D_{\rm cr,sh}$ including the shielding effect by the shell. In each panel, $0.4D_{\rm cr,d}$ and $0.4D_{\rm cr,sh}$ are also shown by a thin solid line and a thin dotted line, respectively.

allow the clouds to collapse if the conditions for $D$ and $n_{\rm on}$ are satisfied. However, in the case of $M_* = 25M_\odot$, ionizing radiation does not help the clouds to collapse, but the fate of clouds is determined solely by $H_2$-dissociating radiation. Hence, we conclude that the critical stellar mass below which ionizing radiation cannot extinguish the negative feedback by photodissociation is $M_* \sim 25M_\odot$.

In Fig. 9, the numerical results are summarized for a low core temperature model ($T_c \sim 200$K). The tendency is qualitatively the same as the results for $T_c \sim 300-400$K. But, the regions of the collapse with the aid of ionizing radiation (triangles) are obviously narrower, and in wider regions the clouds fail to collapse. These results basically originates in the fact that the radius of cloud core is smaller, compared to a high core temperature model with $T_c \sim 300-400$K. For the smaller core radius, $H_2$-dissociating radiation is liable to permeate and suppress the core collapse. However, the critical stellar mass, $M_* \sim 25M_\odot$, below which ionizing radiation cannot extinguish the negative feedback by photodissociation, is almost the same as that in the case with $T_c \sim 400$K. This fact means that the critical stellar mass does not depend sensitively on the cloud core temperature. As a result, we conclude that the critical stellar mass below which ionizing radiation is not important is $M_* \sim 25M_\odot$.

### 4.2 Analytic Criteria

Here, we make analytic estimation of the feedback criteria. Susa (2007) explored the photodissociation feedback of a Pop III star with $120M_\odot$ on a neighboring prestellar core by RHD simulations which dose not include ionizing radiation. Susa (2007) has found that a condition for the collapse of a neighboring core is approximately determined by $t_{\rm dis} = t_{\rm ff}$, where $t_{\rm dis}$ is the photodissociation timescale in the core and $t_{\rm ff}$ is the free-fall timescale. Using the condition, the critical distance $D_{\rm cr,d}$, below which a neighboring core fails to collapse, is given by

$$D_{\rm cr,d} = 147{\rm pc}\left(\frac{L_{\rm LW}}{5\times10^{23}{\rm erg\ s^{-1}}}\right)^{\frac{1}{2}}\left(\frac{n_c}{10^3{\rm cm^{-3}}}\right)^{-\frac{7}{16}} \times\left(\frac{T_c}{300{\rm K}}\right)^{-\frac{3}{4}}, \quad (3)$$

where $L_{\rm LW}$, $n_c$, and $T_c$ are the LW luminosity of source star, the number density of core, and the temperature of core, respectively. This equation involves the self-shielding effect by the core. The dependence on the core temperature basically originates in the core radius ($\propto T_c^{1/2}$) and the $H_2$ formation rate in the core ($\propto T_c$). Hence, the self-shielding effect is weaker for the lower core temperature. As argued in Susa (2007), the boundary between the collapses regardless of ionizing radiation (circles) and with the aid of ionizing radiation (triangles) in Fig. 8 can be roughly explained by $D_{\rm cr,d}$ in the case with $M_* = 120M_\odot$. In addition, as shown in Figs. 8 and 9, $D_{\rm cr,d}$ gives a good estimate for less massive source star cases. However, as shown in Figs. 8, the boundary for the high core temperature model is slightly lower than this analytic estimate. This disagreement can be understand by the dynamical effect of the collapsing clouds

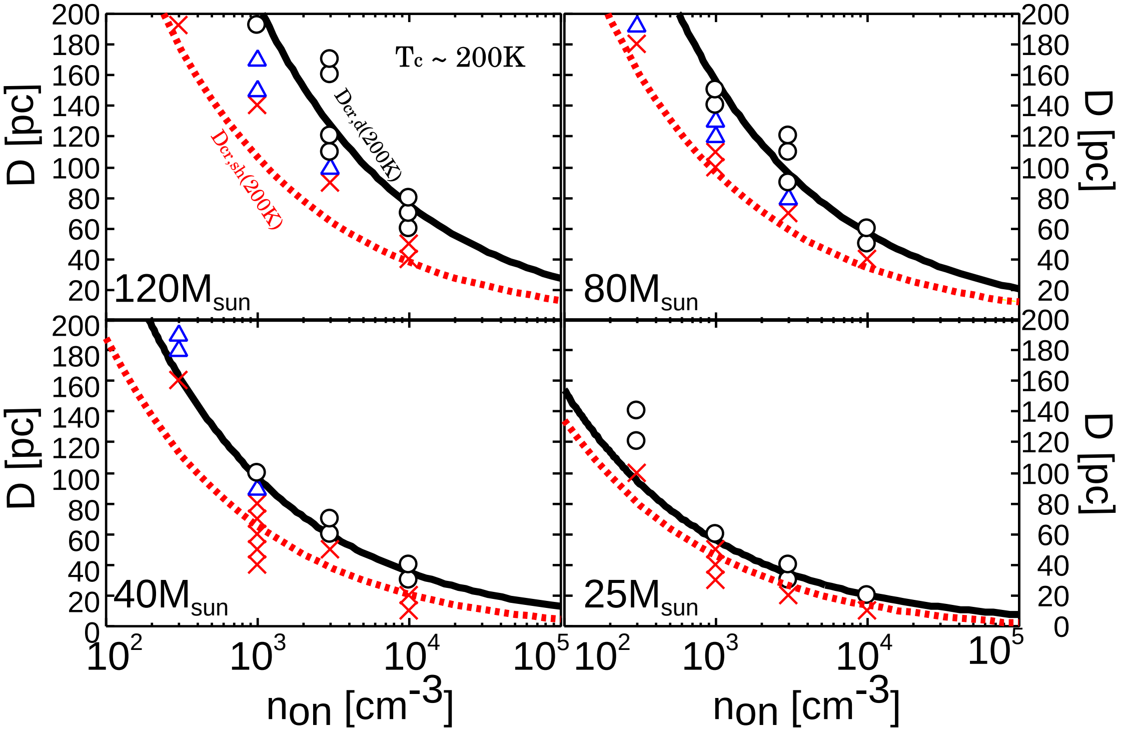

**Figure 9.** Numerical results for $T_c \sim 200$K are summarized in terms of $D$ and $n_{\rm on}$. From the top-left panel to the bottom-right panel, each panel represents the result with $M_* = 120M_\odot$, $80M_\odot$, $40M_\odot$, and $25M_\odot$. Symbols have the same meanings as those in Fig. 8

(Susa 2007). The actual dynamical contraction is faster for the high core temperature model, since the ratio of gravitational energy to internal energy is higher ($|W|/U \approx 4$) as described in §2. Then, the H$_2$ fraction in the core recovers rapidly, during the adiabatic compression phase. Hence, the core can keep collapsing, even if the photodissociation timescale is shorter than the free-fall timescale ($t_{\rm dis} < t_{\rm ff}$) when the cloud irradiated by UV. As a result, the criterion is reduced to $f_{\rm dyn} D_{\rm cr,d}$ by a dynamical factor $f_{\rm dyn}$. Compared to the numerical results, we find $f_{\rm dyn} \approx 0.4$ for the high core temperature model. On the other hand, for the low core temperature model, the dynamical effect is not so strong because of $|W|/U \approx 2$, and therefore $f_{\rm dyn} \approx 1$.

Furthermore, if the ionizing radiation is included, we should incorporate the shielding effect by an H$_2$ shell. Here, we derive a new criterion including the this effect. Since a cloud collapses in a self-similar fashion before UV irradiation, the density profile of outer envelope in the cloud is expressed as

$$n(r) = n_{\rm c} \left(\frac{r_{\rm c}}{r}\right)^2, \tag{4}$$

where $r_{\rm c}$ is the core radius which roughly corresponds to the Jeans scale;

$$r_{\rm c} = \frac{1}{2}\sqrt{\frac{\pi k_B T_{\rm c}}{G m_p^2 n_{\rm c}}}, \tag{5}$$

where $k_{\rm B}$ denotes the Boltzmann constant and $m_{\rm p}$ denotes the proton mass. Assuming that the thickness of the H$_2$ shell is determined by the amount of ionized gas in the envelope and the H$_2$ fraction in the shell is constant, the H$_2$ column density of the shell $N_{\rm H_2,sh}$ is given by

$$N_{\rm H_2,sh} = \int_D^{D_{\rm sh}} y_{\rm H_2,sh} n(r) dr = y_{\rm H_2,sh} n_{\rm c} r_{\rm c}^2 \frac{D - D_{\rm sh}}{D D_{\rm sh}}, \tag{6}$$

where $D_{\rm sh}$, and $y_{\rm H_2,sh}$ are the distance between the cloud core and the H$_2$ shell, and the H$_2$ fraction in the shell, respectively. Here, $D_{\rm sh}$ is set to be the position where the number of recombination per unit time in the ionized region around a source star balances with the number rate of incident ionizing photons, since the H$_2$ shell appears ahead of ionization front. Hence, $D_{\rm sh}$ satisfies

$$\begin{aligned} \frac{N_{\rm ion} \pi D_{\rm sh}^2}{4\pi (D - D_{\rm sh})^2} &= 2\pi\alpha_{\rm B} \int_D^{D_{\rm sh}} n(r)^2 r^2 dr \\ &= 2\pi\alpha_{\rm B} n_c^2 r_c^4 \frac{D - D_{\rm sh}}{D D_{\rm sh}}, \end{aligned} \tag{7}$$

where $\alpha_{\rm B}$ is the recombination coefficient to all excited levels of hydrogen. Using equation (6) and (7), we obtain

$$N_{\rm H_2,sh} = y_{\rm H_2,sh} n_{\rm c}^{\frac{1}{3}} r_{\rm c}^{\frac{2}{3}} D^{-\frac{2}{3}} \left(\frac{N_{\rm ion}}{8\pi\alpha_{\rm B}}\right)^{\frac{1}{3}} \tag{8}$$

Because of the intense LW radiation, the H$_2$ at the shell is in chemical equilibrium. Therefore, $y_{\rm H_2,sh}$ is given by

$$y_{\rm H_2,sh} = \frac{n(D_{\rm sh}) y_{\rm e,sh} k_{\rm H^-}}{k_{\rm dis}}, \tag{9}$$

where $y_{\rm e,sh}$ is the electron fraction at the H$_2$ shell and $k_{\rm H^-}$ is the reaction rate of H$^-$ process. In this case, we should consider the self-shielding effect by the shell itself. As a result, these rates are

$$k_{\rm H^-} = 1.0 \times 10^{-18} T_{\rm sh} {\rm cm^{-3} s^{-1}}, \tag{10}$$

$$k_{\rm dis} = 1.13 \times 10^8 F_{\rm LW,sh} f_{\rm s} \left( \frac{N_{\rm H_2,sh}/2}{10^{14}{\rm cm}^{-2}} \right) {\rm s}^{-1}, \quad (11)$$

where $T_{\rm sh}$ and $F_{\rm LW,sh}$ are the temperature at the shell, and the LW flux from the star in the absence of shielding effect, $F_{\rm LW,sh} = L_{\rm LW}/4\pi(D - D_{\rm sh})^2$. In addition, $f_{\rm s}$ is the self-shielding function given by (2). Combining equations (8)-(11) with assumption of $y_{\rm e,sh} = 0.05$ and $T_{\rm sh} = 2000{\rm K}$ as shown in the present numerical results, we have

$$\begin{aligned} y_{\rm H_2,sh} &= 1.0 \times 10^{-6} \left( \frac{N_{\rm ion}}{10^{50}{\rm s}^{-1}} \right)^{\frac{11}{3}} \left( \frac{L_{\rm LW}}{5 \times 10^{23}{\rm erg\ s}^{-1}} \right)^{-4} \\ &\quad \times \left( \frac{T_{\rm c}}{300{\rm K}} \right)^{-\frac{1}{3}} \left( \frac{D}{40{\rm pc}} \right)^{\frac{2}{3}}, \end{aligned} \quad (12)$$

$$\begin{aligned} N_{\rm H_2,sh} &= 5.8 \times 10^{14} \left( \frac{N_{\rm ion}}{10^{50}{\rm s}^{-1}} \right)^{4} \\ &\quad \times \left( \frac{L_{\rm LW}}{5 \times 10^{23}{\rm erg\ s}^{-1}} \right)^{-4} {\rm cm}^{-2}. \end{aligned} \quad (13)$$

Notice that $N_{\rm H_2,sh}$ is determined solely by the ratio of $N_{\rm ion}$ to $L_{\rm LW}$, and strongly depends on the ratio. In the above numerical results, it is shown that the critical stellar mass does not depend sensitively on the cloud core temperature. This fact is consistent with equation (13), in which the $H_2$ column density of shell is independent of the core temperature $T_{\rm c}$.

Multiplying $L_{\rm LW}$ in equation (3) by $f_{\rm s,sh} \equiv f_{\rm s}\left(\frac{N_{\rm H_2,sh}}{10^{14}{\rm cm}^{-2}}\right)$, we obtain the critical distance as

$$\begin{aligned} D_{\rm cr,sh} &= 147{\rm pc} \left( \frac{L_{\rm LW} f_{\rm s,sh}}{5 \times 10^{23}{\rm erg\ s}^{-1}} \right)^{\frac{1}{2}} \left( \frac{n_{\rm c}}{10^3{\rm cm}^{-3}} \right)^{-\frac{7}{16}} \\ &\quad \times \left( \frac{T_{\rm c}}{300{\rm K}} \right)^{-\frac{3}{4}}, \end{aligned} \quad (14)$$

in which both shielding effects by the core and the $H_2$ shell are taken into account. In particular, when $N_{\rm H_2,sh} > 10^{14}{\rm cm}^{-2}$, the critical distance can be expressed as

$$\begin{aligned} D_{\rm cr,sh} &= 78.8{\rm pc} \left( \frac{L_{\rm LW}}{5 \times 10^{23}{\rm erg\ s}^{-1}} \right)^{2} \left( \frac{N_{\rm ion}}{10^{50}{\rm s}^{-1}} \right)^{-\frac{3}{2}} \\ &\quad \times \left( \frac{n_{\rm c}}{10^3{\rm cm}^{-3}} \right)^{-\frac{7}{16}} \left( \frac{T_{\rm c}}{300{\rm K}} \right)^{-\frac{3}{4}}. \end{aligned} \quad (15)$$

In Fig. 8 and Fig. 9, triangles are the collapse with the aid of an $H_2$ shell. Therefore, the boundary between the triangles and the crosses should be compared with $D_{\rm cr,sh}$. According to equation (13), the shielding effect by the shell becomes weaker according as $N_{\rm ion}/L_{\rm LW}$ decreases. This indicates that $D_{\rm cr,sh}$ approaches $D_{\rm cr,d}$ as the mass of source star becomes lower. As shown in Fig. 8, $D_{\rm cr,sh}$ is the almost same as $D_{\rm cr,d}$ in the case with $M_* = 25M_\odot$. This result originate in the strong dependence of the shell $H_2$ column density on $N_{\rm ion}/L_{\rm LW}$ (see equation 13). As shown in Figs. 8 and 9, $D_{\rm cr,sh}$ gives a qualitatively good estimate for the collapse with the aid of an $H_2$ shell. However, the boundary in Figs. 8 is slightly lower than this analytic estimate. For the same reason as in the case of $D_{\rm cr,d}$, the dynamical effect is more prominent for the high core temperature model. In this case, $f_{\rm dyn} D_{\rm cr,sh}$ with $f_{\rm dyn} \approx 0.4$ provides a more appropriate criterion. On the other hand, for the low core temperature model, $f_{\rm dyn} \approx 1$ gives a plausible criterion.

## 5 CONCLUSIONS AND DISCUSSION

We have carried out RHD simulations to investigate the impact of UV radiation from a Pop III star on nearby collapsing cores. In particular, our attention has been paid to the dependence of UV feedback on the mass of Pop III star. The radiation hydrodynamic evolution of cloud core is determined by not only $H_2$-dissociating radiation but also ionizing radiation. As a result, we have found the critical stellar mass $M_* \approx 25M_\odot$, above which an $H_2$ shell ahead of ionizing front can help clouds to collapse. Owing to the fact that $H_2$-dissociating radiation becomes predominant for less massive source stars, the critical distance for the collapse of a neighboring core does not so strongly depend on the mass of source star. Also, we have derived analytically the feedback criterion, $f_{\rm dyn} D_{\rm cr,sh}$, where $D_{\rm cr,sh}$ is given by (14) and $f_{\rm dyn}$ is a dynamical factor dependent on the the ratio of gravitational energy $W$ to internal energy $U$ of collapsing cloud. We have found $f_{\rm dyn} \approx 0.4$ for $|W|/U \approx 4$, and $f_{\rm dyn} \approx 1$ for $|W|/U \approx 2$. Since $f_{\rm dyn}$ is dependent on $|W|/U$, a dark matter (DM) halo can influence the feedback criterion to a certain degree. In order to assess the effects of DM, we have calculated several models with a static NFW-type dark matter halo potential (Navarro, Frenk & White 1997) with $M_{\rm vir} = 4.15 \times 10^5 M_\odot$ and $r_{\rm vir} = 160{\rm pc}$. In these runs, the ratios of DM mass ($M_{\rm DM}$) to baryonic mass ($M_{\rm b}$) at the central regions of $r < 10{\rm pc}$ are $M_{\rm DM}/M_{\rm b} \simeq 0.3$ for $n_{\rm on} = 10^3{\rm cm}^{-3}$, and $M_{\rm DM}/M_{\rm b} \simeq 1$ for $n_{\rm on} = 10^2{\rm cm}^{-3}$. As a result, we have found that the feedback criterion in the form of $f_{\rm dyn} D_{\rm cr,sh}$ turns out to be still valid, and $f_{\rm dyn}$ becomes smaller by a factor of 1.2 for $n_{\rm on} = 10^3{\rm cm}^{-3}$ and by a factor of 2 for $n_{\rm on} = 10^2{\rm cm}^{-3}$. Therefore, our main results are not changed so much by including DM. Note that the DM density evolution is not treated consistently with the gas dynamics in these simulations. If the DM dynamics is solved with the evolution of gas clouds, the evolutionary path of core temperature might be changed. Hence, for a more quantitative argument, the self-consistent treatment of dark matter would be requisite.

In this paper, we have not considered the lifetime of source stars. The lifetime of Pop III star is $2.5 \times 10^6{\rm yr}$ for $120M_\odot$, $3.0 \times 10^6{\rm yr}$ for $80M_\odot$, $3.9 \times 10^6{\rm yr}$ for $40M_\odot$, and $6.5 \times 10^6{\rm yr}$ for $25M_\odot$ (Schaerer 2002). If the lifetime of source star is shorter than the free-fall time determined by $n_{\rm on}$, the feedback may be significantly changed before the cloud collapse. The density in which the free-fall time equals the stellar lifetime is $n_{\rm on} = 419{\rm cm}^{-3}$ for $120M_\odot$, $n_{\rm on} = 293{\rm cm}^{-3}$ for $80M_\odot$, $n_{\rm on} = 178{\rm cm}^{-3}$ for $40M_\odot$, and $n_{\rm on} = 64{\rm cm}^{-3}$ for $25M_\odot$. Below these densities, arguments including the effects from the stellar lifetime are requisite.

The fate of Pop III stars depends on the mass (Heger & Woosley 2002; Heger et al. 2003). Pop III stars with $120M_\odot$ or $80M_\odot$ may result in direct collapse to black holes (BHs), while those with $40M_\odot$ or $25M_\odot$ may undergo Type II supernova explosions. In the case of direct BH formation, UV source disappears abruptly, and then already-formed $H_2$ molecules can promote the collapse of cloud cores (e.g., Nagakura & Omukai 2005; Johnson & Bromm 2006; Greif & Bromm 2006; Yoshida, Omukai & Hernquist 2007a). In the case of Type II SN explosions, shock-driven hydrodynamic feedbacks could be significant

(Mori et al. 2002; Bromm et al. 2003; Kitayama & Yoshida 2005; Greif et al. 2007).

## ACKNOWLEDGEMENTS

Numerical simulations have been performed with computational facilities at Center for Computational Sciences in University of Tsukuba. This work was supported in part by the *FIRST* project based on Grants-in-Aid for Specially Promoted Research by MEXT (16002003) and Grant-in-Aid for Scientific Research (S) by JSPS (20224002), and also in part by Inamori Research Foundation.

## REFERENCES

Abel T., Bryan G. L., Norman M. L., 2000, ApJ, 540, 39
Ahn K., Shapiro P. R., 2007, MNRAS, 375, 881
Bromm V., Coppi P. S., Larson R. B., 2002, ApJ, 564, 23
Bromm V., Yoshida N., Hernquist L., 2003, ApJ, 596, L135
Cen R., 2003, ApJ, 591, L5
Ciardi B., Ferrara A., Marri S., Raimondo G., 2001, MNRAS, 324, 381
Draine B. T., Bertoldi F., 1996, ApJ, 468, 269
Fuller T. M., Couchman H. M. P., 2000, ApJ 544, 6
Galli D., Palla F., 1998, A & A, 335, 403
Glover S. C. O., Brand P. W. J. L., 2001, MNRAS, 321, 385
Gnedin N. Y., 2000, ApJ, 535, 530
Greif T. H., Bromm V., 2006, MNRAS,373, 128
Greif T. H., Johnson J. L., Bromm V., Klessen R. S., 2007, ApJ, 670, 1
Haiman Rees, M. J., Loeb A., 1997, ApJ, 476, 458
Heger A., Fryer C. L., Woosley S. E., Langer N., Hartmann D. H., 2003, ApJ, 591, 288
Heger A., Woosley S. E., 2002, ApJ, 567, 532
Iwamoto N., Umeda H., Tominaga N., Nomoto K., Maeda K. 2005, Science, 309, 451
Johnson J. L., Bromm V., 2006, MNRAS, 366, 247
Johnson J. L., Greif T. H., Bromm, V., 2008, MNRAS, 694
Kang H., Shapiro P., ApJ, 386, 432
Kitayama T., Susa H.,Umemura M., Ikeuchi S., 2001, MNRAS, 326, 1353
Kitayama T., Yoshida N., 2005, ApJ, 630, 675
Machacek M.E., Bryan G. L., Abel T., 2001, ApJ, 548, 509
Mori M., Ferrara A., Madau P., 2002, ApJ, 571, 40
Nagakura T., Omukai K., 2005, MNRAS, 364, 1378
Nakamoto T., Umemura M., Susa H., 2001, MNRAS, 321, 593
Nakamura F., Umemura M., 2001, ApJ, 548, 19
Nakamura F., Umemura M., 2002, ApJ, 569, 549
Navarro J. F., Frenk C. S., & White S. D. M., 1997, ApJ, 490, 493
Oh S. P., Haiman Z., 2002, ApJ, 569, 558
Omukai K., Nishi R., 1999, ApJ, 518, 64
O'Shea B. W., Norman M. L., 2007, ApJ, 654, 66
O'Shea B. W., Norman M. L., 2008, ApJ, 673, 14
Ricotti M., Gnedin N. Y., Shull, M., 2001, ApJ, 560, 580
Schaerer D., 2002, A&A, 382, 28
Shapiro P. R., Kang H., 1987, ApJ, 318, 32
Sokasian A., Yoshida N., Abel T., Hernquist L., Springel V., 2004, MNRAS, 350, 47
Susa H., 2006, PASJ, 58, 455
Susa H., 2007, ApJ, 659, 908
Susa H., Uehara H., Nishi R., Yamada M., 1998, PThPh, 100, 63
Susa H., Umemura M., 2004, ApJ, 600, 1
Susa H., Umemura M., 2004, ApJ, 610, L5
Susa H., Umemura M., 2006, ApJ, 645, L93
Susa H., Umemura M., Hasegawa K., 2008, in preparation
Tajiri Y., Umemura M., 1998, ApJ, 502, 59
Tegmark M., Silk J., Rees M. J., Blanchard A., Abel T., Palla F., 1997, ApJ, 474, 1
Tornatore L., Ferrara A., Schneider R., 2007, MNRAS, 382, 945
Thoul A. A., Weinberg D. H., 1996, ApJ, 465, 608
Ueharam H., Inutsuka S., 2000, ApJ, 531, L91
Umemura M., Ikeuchi S., 1984, PThPh, 72, 47
Umemura M., Susa H., Suwa T., Sato D., FIRST Project Team, 2007, *First Stars III* (Eds. O'Shea, B.W., Heger, A., & Abel, T.), 386
Umeda H., Nomoto K., 2003, Nature, 422, 871
Whalen D., O'Shea B. W., Smidt J., Norman M. L., 2008, ApJ, 679, 925
Wise J. H., Ablel T., 2008, ApJ, 685, 40
Yoshida N., Abel T., Hernquist L., Sugiyama N., 2003, ApJ, 592, 645
Yoshida N., Omukai K., Hernquist L., Abel, T., 2006, ApJ, 652, 6
Yoshida N., Omukai K., Hernquist L., 2007, ApJ, 667, L117
Yoshida N., Oh S. P., Kitayama T., Hernquist L., 2007, ApJ, 663, 687